



This discussion paper is/has been under review for the journal Hydrology and Earth System Sciences (HESS). Please refer to the corresponding final paper in HESS if available.

# HydroSCAPE: a multi-scale framework for streamflow routing in large-scale hydrological models

S. Piccolroaz<sup>1</sup>, M. Di Lazzaro<sup>2</sup>, A. Zarlenga<sup>2</sup>, B. Majone<sup>1</sup>, A. Bellin<sup>1</sup>, and A. Fiori<sup>2</sup>

<sup>1</sup>Department of Civil, Environmental, and Mechanical Engineering, University of Trento, via Mesiano 77, 38122 Trento, Italy

<sup>2</sup>Department of Engineering, Roma Tre University, Via Vito Volterra 62, 00146 Rome, Italy

Received: 24 August 2015 – Accepted: 26 August 2015 – Published: 4 September 2015

Correspondence to: S. Piccolroaz (s.piccolroaz@unitn.it)

Published by Copernicus Publications on behalf of the European Geosciences Union.

HESSD

12, 9055–9090, 2015

HydroSCAPE: an  
innovative  
multi-scale routing  
model

S. Piccolroaz et al.

Title Page

Abstract

Introduction

Conclusions

References

Tables

Figures



Back

Close

Full Screen / Esc

Printer-friendly Version

Interactive Discussion



## Abstract

We present HydroSCAPE, a large scale hydrological model with an innovative stream-flow routing scheme based on the Width Function Instantaneous Unit Hydrograph (WFIUH) theory, which is designed to facilitate coupling with weather forecasting and climate models. HydroSCAPE preserves geomorphological dispersion of the river network when dealing with horizontal hydrological fluxes, irrespective of the adopted grid size, which is typically inherited from the overlaying weather forecast or climate model. This is achieved through a separate treatment of hillslope processes and routing within the river network, with the latter simulated by suitable transfer functions constructed by applying the WFIUH theory to the desired level of detail. Transfer functions are constructed for each grid cell and nodes of the network where water discharge is desired by taking advantage of the detailed morphological information contained in the Digital Elevation Model of the zone of interest. These characteristics render HydroSCAPE well suited for multi-scale applications, ranging from catchment up to continental scale, and to investigate extreme events (e.g. floods) that require an accurate description of routing through the river network. The model enjoys reliability and robustness, united to parsimony in the adopted parametrization and computational efficiency, leading to a dramatic reduction of the computational effort with respect to full-gridded models at comparable level of accuracy of routing. Additionally, HydroSCAPE is designed with a simple and flexible modular structure, which makes it particularly suitable to massive parallelization, customization according to the specific user needs and preferences (e.g. choice of rainfall-runoff model), and continuous development and improvements.

## 1 Introduction

The emerging of socio-hydrology as a research area of hydrological sciences, addressing multiple scale feedbacks between human activities and hydrological processes, fostered new developments in large-scale hydrological models as a component of more

**HESSD**

12, 9055–9090, 2015

### HydroSCAPE: an innovative multi-scale routing model

S. Piccolroaz et al.

Title Page

Abstract

Introduction

Conclusions

References

Tables

Figures



Back

Close

Full Screen / Esc

Printer-friendly Version

Interactive Discussion







# HESSD

12, 9055–9090, 2015

## HydroSCAPE: an innovative multi-scale routing model

S. Piccolroaz et al.

[Title Page](#)

[Abstract](#)

[Introduction](#)

[Conclusions](#)

[References](#)

[Tables](#)

[Figures](#)



[Back](#)

[Close](#)

[Full Screen / Esc](#)

[Printer-friendly Version](#)

[Interactive Discussion](#)



Mixed schemes in which routing is separated from runoff have also been employed (see e.g. Gong et al., 2009, 2011; Wen et al., 2012; Lehner and Grill, 2013). HydroROUT is a vector-based routing scheme fully integrated with ArcGIS (ESRI, 2011) developed by Lehner and Grill (2013), in which streamflow is obtained by routing to the catchment outlet the surface runoff (as provided by an external runoff simulator to be coupled with the routing scheme) accumulated at the nodes of the network. Routing is performed by using a “plug-flow” routing scheme similar to that implemented by Whiteaker et al. (2006) and applied to the HydroSHEDS river network (Lehner et al., 2006).

Wen et al. (2012) proposed a multi-scale routing framework employing a pdf distribution for the overland flow path lengths lumping the effect of unmodeled sub-grid variability in the parameters describing the pdf. The kinematic wave routing method is then employed for both overland and channel flow simulations, thereby resulting in a highly computational demand, as already discussed above. In addition, the routing scheme generates streamflow only at the outlet of the catchment without the possibility to simulate streamflows at internal nodes, such as lakes, reservoirs or other infrastructures, while the use of response functions aggregated at the daily time scale limits the applicability to flood events occurring in large river basins, with the approach proposed by Gong et al. (2009, 2011).

To overcome the above limitations without resorting to hyper resolution hydrological models (when not needed to better reproduce spatial variability of soil water storage and transmission), we propose a multi-scale approach for streamflow routing based on the travel time approach. More specifically, we propose a scheme based on the Width-Function Instantaneous Unit Hydrograph (WFIUH) theory (see e.g. Rodríguez-Iturbe and Rinaldo, 1997), applied to a hybrid raster-vector data structure, according to the definition proposed by Lehner and Grill (2013). To emphasize that the model is designed to reproduce the effect of landscape on horizontal water transfer, we coined the name “HydroSCAPE”, where “SCAPE” also recalls that the model is inherently SCAlable and highly Parallelizable. In fact, by design, routing is independent from the







of the domain into macrocells may be arbitrary (i.e. it does not necessarily use topographic information).

The next step in the construction of the model is the identification of the  $N_k$  nodes where streamflow is desired. In the example of Fig. 1,  $N_k = 5$  nodes, identified by red bullets, are distributed within two networks. No limitations are imposed to the number and position of these nodes, which represent locations where streamflow is computed either to compare it with observational data, as part of the inversion procedure, or for other purposes, such as to verify flood protection structures (or the need to build them). Each macrocell  $i$  may feed one or more nodes; for instance, the macrocell  $i = 3$  in Fig. 1 includes contributing areas to nodes  $k = 1$  and  $k = 2$ , with different routes. It may also occur that a macrocell contributes to the same node  $k$  with different routes, as for the case of macrocell  $i = 2$  which contributes to node  $k = 1$ , through both hillslopes highlighted in green and brown.

We denote with  $A_k^{(i)}$  the area of macrocell  $i$  contributing to node  $k$ , such that  $\sum_{k=1}^{N_k} A_k^{(i)} = A^{(i)}$ . Notice that  $A_k^{(i)} = 0$  if the macrocell  $i$  does not contribute to node  $k$ . The streamflow generation processes occurring at the hillslope scale can be modeled by using schemes of different level of complexity, from the simple SCS-CN method (US Soil Conservation Service, 1964) to methods based on the solution of the Richards equation, or one of its simplification (Clark et al., 2015), depending on the objectives of the analysis. Whatever the hillslope model, hereafter we indicate with  $\eta_{\ell k}^{(i)}$  [ $\text{L T}^{-1}$ ] the water discharge per unit area produced by the hillslope  $\ell$  of area  $a_{\ell k}^{(i)}$  [ $\text{L}^2$ ], which belongs to the macrocell  $i$  and contributes to the streamflow at the closest downstream node  $k$  along the river network (for instance, the hillslope highlighted in green in Fig. 1 contributes to node  $k = 1$ , which is the first node encountered moving downstream). The resulting water flow depends on the partitioning of hydrological fluxes, triggered by rain-fall or snowmelt, at the hillslope scale and may include the contribution of groundwater. According to the above conceptual scheme, water flow produced by the hillslope enters

**HydroSCAPE: an  
innovative  
multi-scale routing  
model**

S. Piccolroaz et al.

Title Page

Abstract

Introduction

Conclusions

References

Tables

Figures

◀

▶

◀

▶

Back

Close

Full Screen / Esc

Printer-friendly Version

Interactive Discussion





the network system through the hillslope-channel transition site, and is subsequently routed through it.

From this kinematic scheme, it follows that the streamflow contribution of the hillslope  $\ell$ , belonging to the macrocell  $i$ , to node  $k$  can be written as follows

$$q_{\ell k}^{(i)}(t) = A_k^{(i)} \tilde{a}_{\ell k}^{(i)} \int_0^t \eta_{\ell k}^{(i)}(t - \tau) \delta[\tau - \tau_{\ell k}^{(i)}] d\tau = A_k^{(i)} \tilde{a}_{\ell k}^{(i)} \eta_{\ell k}^{(i)}(t - \tau_{\ell k}^{(i)}), \quad (1)$$

where  $\tilde{a}_{\ell k}^{(i)} = a_{\ell k}^{(i)} / A_k^{(i)}$  [-] is the relative hillslope area,  $\delta$  [1/T] is the Dirac delta function,  $\tau_{\ell k}^{(i)}$  [T] is the travel time from the hillslope-channel transition site of the hillslope  $\ell$  to node  $k$ , and  $t$  [T] is the current time.

Under the hypothesis that the stream velocity  $V_c$  [ $L T^{-1}$ ] is constant through the network, the travel time assumes the following expression:  $\tau_{\ell k}^{(i)} = L_{\ell k}^{(i)} / V_c$ , where  $L_{\ell k}^{(i)}$  is the distance, measured along the network, from the hillslope-channel transition site of the hillslope  $\ell$  to the first downstream node  $k$ . The assumption of constant  $V_c$  is crucial for the linearity of the processes at the watershed scale, as stated at the beginning of this section. Equation (1) is consistent with the general conceptual framework used to derive the Width Function Instantaneous Unitary Hydrograph by rescaling the geomorphological width function through a suitable constant velocity (Gupta et al., 1986; Mesa and Mifflin, 1986; Gupta and Mesa, 1988; Rodríguez-Iturbe and Rinaldo, 1997). In agreement with the WFIUH theory, stream hydrodynamic dispersion is neglected, owing to its small to negligible effect on the hydrological response, which has been demonstrated to be dominated by geomorphological dispersion already embedded into the rescaled width function (Rinaldo et al., 1991, 1995; Rodríguez-Iturbe and Rinaldo, 1997).

The streamflow  $q_k^{(i)}$  [ $L^3 T^{-1}$ ] generated by macrocell  $i$  and contributing to the node  $k$  is then obtained by summing up all the contributions stemming from the hillslopes of the macrocell draining to the node  $k$ :

**HydroSCAPE: an innovative multi-scale routing model**

S. Piccolroaz et al.

Title Page

Abstract

Introduction

Conclusions

References

Tables

Figures

⏪

⏩

◀

▶

Back

Close

Full Screen / Esc

Printer-friendly Version

Interactive Discussion



$$q_k^{(i)}(t) = A_k^{(i)} \sum_{\ell} \tilde{a}_{\ell k}^{(i)} \int_0^t \eta_{\ell k}^{(i)}(t - \tau) \delta[\tau - \tau_{\ell k}^{(i)}] d\tau. \quad (2)$$

Under the hypothesis that the hillslope water discharge per unit area is constant through the cell  $i$ , i.e. by assuming that  $\eta_{\ell k}^{(i)} = \eta^{(i)}$ , Eq. (2) simplifies to:

$$q_k^{(i)}(t) = A_k^{(i)} \int_0^t \eta^{(i)}(t - \tau) f_k^{(i)}(\tau) d\tau = A_k^{(i)} \eta^{(i)} * f_k^{(i)}(t), \quad (3)$$

5 where  $f_k^{(i)}(\tau) = \sum_{\ell} \tilde{a}_{\ell k}^{(i)} \delta[\tau - L_{\ell k}^{(i)}/V_c]$  is the probability density function (pdf) of the travel time  $\tau_{\ell k}^{(i)}$  weighted by the relative hillslope area  $\tilde{a}_{\ell k}^{(i)}$ . In Eq. (3) the asterisk denotes convolution.

10 Finally, water discharge  $Q_k(t)$  [ $L^3 T^{-1}$ ] at the node  $k$  is given by the sum of the direct contribution of each macrocell  $i$  to the node plus the contribution of the nodes upstream of  $k$ :

$$Q_k(t) = \sum_{i=1}^N q_k^{(i)}(t) + \sum_{i=1}^N \sum_{j=1}^{N_k^{\text{up}}} q_j^{(i)}(t - \tau_{jk}), \quad (4)$$

15 where  $\tau_{jk} = D_{jk}/V_c$  is the travel time from the node  $j$ , located upstream to the node  $k$ , to the node  $k$ ,  $D_{jk}$  is the distance between the two nodes, and  $N_k^{\text{up}}$  is the number of nodes upstream of  $k$ . In the first right hand term of Eq. (4) summations are extended over all the macrocells, with the convention that  $q_k^{(i)} = 0$ , because  $A_k^{(i)} = 0$ , for all macrocells not contributing, i.e. not connected through the network, to the node  $k$  (the same applies for index  $j$ ). Notice that, in the second right hand term of Eq. (4) the streamflow

computed at the node  $j$  is rigidly translated to the node  $k$  with the delay  $\tau_{jk}$  depending on the distance between the two nodes, thereby neglecting again the effect of stream hydrodynamic dispersion, as typically done in the WFIUH approach (see e.g. Gupta et al., 1986; Van Der Tak and Bras, 1990; Botter and Rinaldo, 2003; Giannoni et al., 2005).

The above method is simple and computationally effective. The underlying principle is similar to the block-effective dispersion employed in groundwater hydrology (see e.g. Rubin et al., 1999; De Barros and Rubin, 2011), with the travel time pdf used to represent the effect on streamflow of morphological heterogeneity at scales smaller than the macrocell, with a lower cutoff given by the DEM's scale. The linearity of the transfer processes at the scale of the network makes the algorithm easy to parallelize. In principle, streamflow generated by a macrocell can be elaborated by a single processor (with the convolution of Eq. (3) being the most demanding step), for the whole duration of the simulations, independently from the other processors. Then, the streamflow  $Q_k(t)$  at the nodes of interest is further processed with Eq. (4) when all processors terminated the elaboration of their macrocell. For the same reasons, this model is particularly suited to multiple Monte Carlo runs (e.g. for parameter estimation, uncertainty analysis or multi-model or multi-scenario analysis). The main advantage of the method is that, by design, it preserves the global geomorphological dispersion of the basin, as calculated by the fine grid DEM, no matter the size of the macrocells. Consequently, the upscaling of river network dispersion is perfectly resolved, without resorting to hyper-resolution numerical grids. This point shall be illustrated in the ensuing Section. In addition, with the proposed approach we address one of the main limitation of the WFIUH formulation: the inadequacy of the original method (generally based on a single WFIUH for the whole river basin) to properly account for spatial variability of precipitation. It is in fact recognized that at intermediate spatial scale (typically beyond a few thousands of  $\text{km}^2$ ) the spatial distribution of rainfall plays a fundamental role in shaping the hydrological response of river basins (see e.g. Nicótina et al., 2008; Volpi et al., 2012; Sapriza-Azuri et al., 2015). With our approach this limitation is overcome by assembling in the right

## HESSD

12, 9055–9090, 2015

### HydroSCAPE: an innovative multi-scale routing model

S. Piccolroaz et al.

Title Page

Abstract

Introduction

Conclusions

References

Tables

Figures

⏪

⏩

◀

▶

Back

Close

Full Screen / Esc

Printer-friendly Version

Interactive Discussion







gauging stations together with the subdivision of the watershed into the 5 inter-basin areas.

In the following the effect of spatial discretization on the hydrologic response is analyzed with reference to macrocells of different dimensions. In particular, the study area was overlaid with macrocells of increasing size, from 1 to 150 km (the latter including the whole Upper Tiber river basin within a single macrocell), and corresponding to about 37'' and 1°36', respectively. Domain discretization with macrocells of 5, 10 and 50 km are shown as an example in Fig. 4.

Identification of the drainage network and associated geomorphic metrics was performed by adopting standard DEM pre-processing techniques. In particular, the identification of the flow path lengths involved the following steps: (i) pit and flat area removal following the procedure of Tarboton et al. (1991); (ii) determination of the drainage directions by using the standard single direction D8 algorithm (O'Callaghan and Mark, 1984); (iii) identification of the space filling tree network, which connects each site to the outlet; (iv) definition of channel initiation, by adopting a combination of the threshold-slope area and the threshold-support area criteria (Di Lazzaro, 2009).

For a given resolution of the macrocell grid, it is thus possible to derive the frequency distribution  $f_{\ell k}^{(i)}$  of the flow path lengths  $L_{\ell k}^{(i)}$  pertaining to macrocell  $i$  and connecting the hillslope-channel transition site of the hillslope  $\ell$  to the control node  $k$  (i.e. the macrocell-node specific width functions introduced in Sect. 2), which is the best possible approximation of the width function, given the scale of the DEM.

Figure 4 shows as an example width functions constructed at the Santa Lucia node (upstream node on the main river-course, see Fig. 3), for macrocell size of 5 km (Fig. 3a), 10 km (Fig. 3b) and 50 km (Fig. 3c), respectively. We observe that the distribution of path lengths is wider for larger macrocells, because more hillslopes contributing to the node are included into the same macrocell, such that a larger portion of available path lengths is sampled. When a single macrocell is used, containing the entire catchment, all the hillslopes are included and the macrocell width function coincides with that of the catchment. On the other hand, when the macrocell coincides with the cell of

## HESSD

12, 9055–9090, 2015

### HydroSCAPE: an innovative multi-scale routing model

S. Piccolroaz et al.

Title Page

Abstract

Introduction

Conclusions

References

Tables

Figures

⏪

⏩

◀

▶

Back

Close

Full Screen / Esc

Printer-friendly Version

Interactive Discussion







ch. 7.3). This is consistent with the notion that travel times in hillslopes are important in shaping the hydrologic response of a watershed and cannot be neglected even for large river basins, where the channeled lengths are usually much larger than the mean hillslope size (Botter and Rinaldo, 2003; D’Odorico and Rigon, 2003; Di Lazzaro and Volpi, 2011). Subsurface contribution to streamflow was not explicitly considered for this specific model configuration, which is focused on floods. As an alternative to the linear reservoir model, a hillslope scale rescaled width function can be used to represent the travel time distribution at the hillslope scale. In this case, rescaling may be obtained by using a hillslope specific velocity  $V_\ell \ll V_c$ .

At the hillslope scale runoff is computed by using the classic SCS-CN scheme:

$$R_i(t) = \frac{(P_i(t) - I_{a,i})^2}{P_i(t) + c_S S_i - I_{a,i}}, \quad (5)$$

where  $P_i(t)$  [L] and  $R_i(t)$  [L] are the cumulative rainfall and the cumulative runoff, respectively, at time  $t$ , both assumed uniform within the macrocell  $i$ . In addition,  $S_i$  [L] is the soil potential maximum infiltration (identified on the basis of the map of CNII shown in Fig. 2c),  $I_a = \alpha c_S S$  [L] is the initial abstraction, with  $\alpha < 1$  [-] introduced to represent the initial abstraction as a fraction of the maximum infiltration, and  $c_S$  [-] is a multiplicative factor accounting for uncertainty in the identification of  $S$ .

Therefore, the effective rainfall intensity  $p_i$  [ $L T^{-1}$ ] at time  $t$  can be computed as follows:

$$p_i(t) = \frac{R_i(t) - R_i(t - \Delta t)}{\Delta t}, \quad (6)$$

and Eq. (5) is applied at discrete times, according to the time step  $\Delta t$ .

The specific water flux produced by the hillslopes of the macrocell  $i$  can be obtained by applying mass conservation at the hillslope scale by considering the effective precipitation as inflow and runoff  $\eta$  as the only outflow (evapotranspiration can be neglected

## HESSD

12, 9055–9090, 2015

### HydroSCAPE: an innovative multi-scale routing model

S. Piccolroaz et al.

Title Page

Abstract

Introduction

Conclusions

References

Tables

Figures

⏪

⏩

◀

▶

Back

Close

Full Screen / Esc

Printer-friendly Version

Interactive Discussion



since the model is applied at the flood event temporal scale):

$$\frac{\eta^{(i)}(t) - \eta^{(i)}(t - \Delta t)}{\Delta t} = \frac{1}{\lambda} \left[ \rho_i(t) - \eta^{(i)}(t - \Delta t) \right], \quad (7)$$

where  $\lambda$  [T] is the mean residence time of the linear reservoir and the left hand term is the first order approximation of the time derivative of runoff  $\eta^{(i)}$ . Parameters  $\alpha$ ,  $c_S$  and  $\lambda$  were assumed uniform through the river basin, i.e. all the macrocells share the same coefficients. On the basis of preliminary analysis  $\alpha$  was found not to be a sensitive parameter and was set to 0.08 (which is in agreement with the values found by D'Asaro and Grillone, 2012), while  $c_S$  and  $\lambda$  are calibration parameters, together with the channel velocity  $V_c$ . We emphasize that this simplified version of HydroSCAPE is event-based since it does not include a continuous soil-moisture budget; however, this is enough for the purpose of this example application, mainly focused on flood events, which aim is to show how HydroSCAPE implements routing. As explained in Sect. 2, HydroSCAPE is not limited to this simplified implementation, yet effective for the purpose of flood forecasting, and can work with more sophisticated runoff generation schemes.

In order to illustrate model performance we selected two major rainfall events within the decade 1990–2000, that generated significant, yet not extreme, floods. The streamflow triggered by these rainfall events was compared with observational data at the 5 nodes described in Sect. 3.1. The two events occurred in December 1992 and February 1999, respectively. In both cases precipitation was caused by humid frontal advection from the Mediterranean Sea followed by condensation due to orographic uplift (Calenda et al., 2005). The spatial distribution of the precipitation was obtained by interpolation of the measurements at the available rain gauges (18 and 32 for the events of December 1992 and February 1999, respectively) by means of Kriging with External Drift (see e.g. Goovaerts, 1997). The precipitation was interpolated separately at each time step by using the same exponential semivariogram which has been obtained by analyzing offline the available data. In particular, precipitation was first calculated over

HydroSCAPE: an innovative multi-scale routing model

S. Piccolroaz et al.

Title Page

Abstract

Introduction

Conclusions

References

Tables

Figures

⏪

⏩

◀

▶

Back

Close

Full Screen / Esc

Printer-friendly Version

Interactive Discussion





# HESSD

12, 9055–9090, 2015

## HydroSCAPE: an innovative multi-scale routing model

S. Piccolroaz et al.

[Title Page](#)

[Abstract](#)

[Introduction](#)

[Conclusions](#)

[References](#)

[Tables](#)

[Figures](#)



[Back](#)

[Close](#)

[Full Screen / Esc](#)

[Printer-friendly Version](#)

[Interactive Discussion](#)



single processor (Intel(R) Xeon(R) W5580 at 3.20 GHz core), the code being written in Fortran 90, is shown to increase from a few seconds in the case of one single macro-cell to about 10 min for the finer resolution (1 km, corresponding to 476 macrocells). We emphasize that the computational efforts can be reduced considerably by implementing parallel computing techniques, to which HydroSCAPE is particularly suited thanks to its inherently parallel formulation (see also Sect. 2).

Model validation was carried out by means of a combined multi-site, multi-event approach, and was coupled with a Monte Carlo based uncertainty analysis performed on a subset of parameter combinations sampled during calibration at PN with the 1999 flood event as observational data. This subset was identified according to a model efficiency rejection criterion that classifies as behavioral all sets of parameters with a NSE index greater than zero, resulting in 14 958 parameters sets and model realizations. Successively, the 95 % uncertainty bands associated with the retained simulations were evaluated using the standard likelihood weighted procedure proposed by Freer et al. (1996). Results obtained for the 10 km spatial resolution configuration are presented in Fig. 6, which shows 95 % prediction uncertainty bands and observed streamflow at the 5 nodes shown in Fig. 3. Simulated hydrographs obtained adopting the optimal parameter set reported in Table 2 are also shown with a continuous black line. Figure 6a–e show uncertainty bands for the February 1999 event (the calibration event) considering all the gauging stations including PN, which was the only used in calibration. Other indicators of goodness are  $P$  and  $R$  factors (see e.g. Abbaspour et al., 2009), which are defined as the percentage of data bracketed by the confidence band, and the ratio between the average width of the band and the standard deviation of observations, respectively. Computed water discharge at all nodes provided high  $P$  factor values (80 % for SL and 100 % for all the others), and moderate  $R$  factor values (1.99, 2.56, 1.62, 2.87, and 3.21 for PN, PF, SL, PR, and PB, respectively). The somewhat suboptimal performance with respect to the  $R$  factor is in part due to the decision of considering behavioral all the models with  $NSE > 0$ , instead of the typical choice of setting the threshold at  $NSE = 0.5$ , with the consequent reduction of the uncertainty band

thus of the  $R$  factor. Visual inspection of Fig. 6 and the above performance factors indicate that the model is able to encompass most of the observed discharges, while retaining reasonable uncertainty band amplitudes. The same analysis was performed also for the event occurred between 4 and 7 December 1992 (multi-site, multi-event validation). Results are presented in Fig. 6f–i, which suggest reasonable model prediction capability ( $P$  factor equal to 100, 39, 17, 100 %, and  $R$  factor equal to 1.63, 1.47, 1.06, and 2.28, for PN, PF, SL, and PR, respectively; we note that no water discharge data were available at PB during this event), although a general tendency to underestimate the flood volume is evident. This is likely due to inherent differences between precipitation conditions (e.g. intensity, spatial distribution) during the two events and in the preceding days, which reflect into different initial soil moisture conditions that cannot be fully captured with the simple event-based SCS-CN model used here.

## 4 Conclusions

This work presents an innovative, multi-scale streamflow routing method based on the travel time approach. The principal aim is to develop a simple, parsimonious and computationally efficient method for modeling streamflow (and particularly floods) in large basins. The model, coined as HydroSCAPE, aims at correctly reproduce the relevant hydrological fluxes across the scales of interest, from a single catchment to the whole continent. The method is based on the WFIUH theory applied to a hybrid raster-vector data structure, that allows to derive localized information on travel times and flow characteristics without the need of narrowing the resolution of the computational grid adopted for the study area. The relevant features of the model are illustrated through the modeling of two flood events in the Upper Tiber river basin (Central Italy), with 4 different domain discretizations, i.e. different dimensions of macrocells.

The main results of the present work can be summarized as follows:

- HydroSCAPE employs a strategy for modeling cell-scale runoff dispersivity such that the catchment response is independent from the grid size, which in turn is

**HESSD**

12, 9055–9090, 2015

## HydroSCAPE: an innovative multi-scale routing model

S. Piccolroaz et al.

Title Page

Abstract

Introduction

Conclusions

References

Tables

Figures

⏪

⏩

◀

▶

Back

Close

Full Screen / Esc

Printer-friendly Version

Interactive Discussion





## HydroSCAPE: an innovative multi-scale routing model

S. Piccolroaz et al.

[Title Page](#)

[Abstract](#)

[Introduction](#)

[Conclusions](#)

[References](#)

[Tables](#)

[Figures](#)

[⏪](#)

[⏩](#)

[◀](#)

[▶](#)

[Back](#)

[Close](#)

[Full Screen / Esc](#)

[Printer-friendly Version](#)

[Interactive Discussion](#)



We believe that all of the above characteristics make of HydroSCAPE an appealing routing tool to be implemented in LHMs, particularly suitable for climate change impact studies where the accuracy of the streamflow routing may be significantly affected by the spatial resolution adopted.

5 *Acknowledgements.* This research has been partially funded by the Italian Ministry of Public Instruction, University and Research through the project PRIN 2010-2011 (Innovative methods for water resources management under hydro-climatic uncertainty scenarios, prot. 2010JHF437). S. Piccolroaz, B. Majone and A. Bellin were also supported by European Union FP7 Collaborative Project GLOBAQUA (Managing the effects of multiple stressors on aquatic ecosystems under water scarcity, Grant No. 603629-ENV-2013.6.2.1). Authors also thank the Hydrographic Service of Umbria Region for data provision.

## References

- 15 Abbaspour, K. C., Faramarzi, M., Ghasemi, S. S., and Yang, H.: Assessing the impact of climate change on water resources in Iran, *Water Resour. Res.*, 45, W10434, doi:10.1029/2008WR007615, 2009. 9073
- Arnell, N. W.: A simple water balance model for the simulation of streamflow over a large geographic domain, *J. Hydrol.*, 217, 314–335, doi:10.1016/S0022-1694(99)00023-2, 1999. 9057
- Bellin, A., Majone, B., Cainelli, O., Alberici, D., and Villa, F.: GEOTRANSF: A continuous coupled hydrological and water resources management model, *Environ. Modell. Softw.*, in review, 2015. 9066
- 20 Botter, G. and Rinaldo, A.: Scale effect on geomorphologic and kinematic dispersion, *Water Resour. Res.*, 39, SWC61–SWC610, doi:10.1029/2003WR002154, 2003. 9065, 9070
- Calenda, G., Gorgucci, E., Napolitano, F., Novella, A., and Volpi, E.: Multifractal analysis of radar rainfall fields over the area of Rome, *Adv. Geosci.*, 2, 293–299, doi:10.5194/adgeo-2-293-2005, 2005. 9071
- 25 Clark, M. P., Fan, Y., Lawrence, D. M., Adam, J. C., Bolster, D., Gochis, D. J., Hooper, R. P., Kumar, M., Leung, L. R., Mackay, D. S., Maxwell, R. M., Shen, C., Swenson, S. C., and Zeng, X.: Improving the representation of hydrologic processes in Earth System Models, *Water Resour. Res.*, doi:10.1002/2015WR017096, in press, 2015. 9058, 9062



## HydroSCAPE: an innovative multi-scale routing model

S. Piccolroaz et al.

Title Page

Abstract

Introduction

Conclusions

References

Tables

Figures

⏪

⏩

◀

▶

Back

Close

Full Screen / Esc

Printer-friendly Version

Interactive Discussion



D'Asaro, F. and Grillone, G.: Empirical Investigation of Curve Number Method Parameters in the Mediterranean Area, *J. Hydrol. Eng.*, 17, 1141–1152, doi:10.1061/(ASCE)HE.1943-5584.0000570, 2012. 9071

De Barros, F. P. J. and Rubin, Y.: Modelling of block-scale macrodispersion as a random function, *J. Fluid Mech.*, 676, 514–545, doi:10.1017/jfm.2011.65, 2011. 9065

De Paiva, R. C. D., Buarque, D. C., Collischonn, W., Bonnet, M. P., Frappart, F., Calmant, S., and Bulhões Mendes, C. A.: Large-scale hydrologic and hydrodynamic modeling of the Amazon River basin, *Water Resour. Res.*, 49, 1226–1243, doi:10.1002/wrcr.20067, 2013. 9058

Di Lazzaro, M.: Regional analysis of storm hydrographs in the Rescaled Width Function framework, *J. Hydrol.*, 373, 352–365, doi:10.1016/j.jhydrol.2009.04.027, 2009. 9068

Di Lazzaro, M. and Volpi, E.: Effects of hillslope dynamics and network geometry on the scaling properties of the hydrologic response, *Adv. Water Resour.*, 34, 1496–1507, doi:10.1016/j.advwatres.2011.07.012, 2011. 9070

D'Odorico, P. and Rigon, R.: Hillslope and channel contributions to the hydrologic response, *Water Resour. Res.*, 39, SWC11–SWC19, doi:10.1029/2002WR001708, 2003. 9070

Döll, P., Kaspar, F., and Lehner, B.: A global hydrological model for deriving water availability indicators: Model tuning and validation, *J. Hydrol.*, 270, 105–134, doi:10.1016/S0022-1694(02)00283-4, 2003. 9057

ESRI: ArcGIS Desktop: Release 10, Environmental Systems Research Institute, Redlands, CA, USA, <http://www.esri.com/software/arcgis/arcgis-for-desktop> (last access: 15 July 2015), 2011. 9059

Freer, J., Beven, K., and Ambrose, B.: Bayesian estimation of uncertainty in runoff prediction and the value of data: An application of the GLUE approach, *Water Resour. Res.*, 32, 2161–2173, doi:10.1029/95WR03723, 1996. 9073

Giannoni, F., Roth, G., and Rudari, R.: A procedure for drainage network identification from geomorphology and its application to the prediction of the hydrologic response, *Adv. Water Resour.*, 28, 567–581, doi:10.1016/j.advwatres.2004.11.013, 2005. 9065

Gong, L., Widén-Nilsson, E., Halldin, S., and Xu, C. Y.: Large-scale runoff routing with an aggregated network-response function, *J. Hydrol.*, 368, 237–250, doi:10.1016/j.jhydrol.2009.02.007, 2009. 9058, 9059

Gong, L., Halldin, S., and Xu, C. Y.: Global-scale river routing-an efficient time-delay algorithm based on HydroSHEDS high-resolution hydrography, *Hydrol. Process.*, 25, 1114–1128, doi:10.1002/hyp.7795, 2011. 9059

- Goovaerts, P.: Geostatistics for natural resources evaluation, University Press, Oxford, USA, 1997. 9071
- Gupta, V. K. and Mesa, O. J.: Runoff generation and hydrologic response via channel network geomorphology – recent progress and open problems, *J. Hydrol.*, 102, 3–28, doi:10.1016/0022-1694(88)90089-3, 1988. 9063
- Gupta, V. K., Waymire, E., and Rodríguez-Iturbe, I.: On Scales, Gravity and Network Structure in Basin Runoff, in: *Scale Problems in Hydrology*, vol. 6 Water Science and Technology Library, edited by: Gupta, V. K., Rodríguez-Iturbe, I., and Wood, E. F., Springer Netherlands, 159–184, doi:10.1007/978-94-009-4678-1\_8, 1986. 9063, 9065
- Haddeland, I., Clark, D. B., Franssen, W., Ludwig, F., Voß, F., Arnell, N. W., Bertrand, N., Best, M., Folwell, S., Gerten, D., Gomes, S., Gosling, S. N., Hagemann, S., Hanasaki, N., Harding, R., Heinke, J., Kabat, P., Koirala, S., Oki, T., Polcher, J., Stacke, T., Viterbo, P., Weedon, G. P., and Yeh, P.: Multimodel estimate of the global terrestrial water balance: Setup and first results, *J. Hydrometeorol.*, 12, 869–884, doi:10.1175/2011JHM1324.1, 2011. 9057
- Hanasaki, N., Kanae, S., Oki, T., Masuda, K., Motoya, K., Shirakawa, N., Shen, Y., and Tanaka, K.: An integrated model for the assessment of global water resources – Part 1: Model description and input meteorological forcing, *Hydrol. Earth Syst. Sci.*, 12, 1007–1025, doi:10.5194/hess-12-1007-2008, 2008a. 9057
- Hanasaki, N., Kanae, S., Oki, T., Masuda, K., Motoya, K., Shirakawa, N., Shen, Y., and Tanaka, K.: An integrated model for the assessment of global water resources – Part 2: Applications and assessments, *Hydrol. Earth Syst. Sci.*, 12, 1027–1037, doi:10.5194/hess-12-1027-2008, 2008b. 9057
- Kavvas, M. L., Kure, S., Chen, Z. Q., Ohara, N., and Jang, S.: WEHY-HCM for Modeling Interactive Atmospheric-Hydrologic Processes at Watershed Scale, I: Model Description, *J. Hydrol. Eng.*, 18, 1262–1271, doi:10.1061/(ASCE)HE.1943-5584.0000724, 2013. 9057
- Lehner, B. and Grill, G.: Global river hydrography and network routing: Baseline data and new approaches to study the world's large river systems, *Hydrol. Process.*, 27, 2171–2186, doi:10.1002/hyp.9740, 2013. 9059
- Lehner, B., Verdin, K., and Jarvis, A.: *HydroSHEDS Technical Documentation, Version 1.0*, Tech. rep., World Wildlife Fund US, Washington, D.C., available at: <http://hydrosheds.cr.usgs.gov> (last access: 15 July 2015), 2006. 9059

---

**HydroSCAPE: an innovative multi-scale routing model**S. Piccolroaz et al.

---

[Title Page](#)[Abstract](#)[Introduction](#)[Conclusions](#)[References](#)[Tables](#)[Figures](#)[⏪](#)[⏩](#)[◀](#)[▶](#)[Back](#)[Close](#)[Full Screen / Esc](#)[Printer-friendly Version](#)[Interactive Discussion](#)

## HydroSCAPE: an innovative multi-scale routing model

S. Piccolroaz et al.

[Title Page](#)

[Abstract](#)

[Introduction](#)

[Conclusions](#)

[References](#)

[Tables](#)

[Figures](#)

[⏪](#)

[⏩](#)

[◀](#)

[▶](#)

[Back](#)

[Close](#)

[Full Screen / Esc](#)

[Printer-friendly Version](#)

[Interactive Discussion](#)



- Lehner, B., Verdin, K., and Jarvis, A.: New global hydrography derived from spaceborne elevation data, *EOS Trans. Am. Geophys. Union*, 89, 93–94, doi:10.1029/2008EO100001, 2008. 9058
- Liang, X., Lettenmaier, D. P., Wood, E. F., and Burges, S. J.: A simple hydrologically based model of land surface water and energy fluxes for general circulation models, *J. Geophys. Res.-Atmos.*, 99, 14415–14428, doi:10.1029/94JD00483, 1994. 9057
- Manabe, S.: Climate and the ocean circulation: 1. The atmospheric circulation and the hydrology of the Earth's surface, *Mon. Weather Rev.*, 97, 739–805, 1969. 9057
- Manfreda, S., Nardi, F., Samela, C., Grimaldi, S., Taramasso, A. C., Roth, G., and Sole, A.: Investigation on the use of geomorphic approaches for the delineation of flood prone areas, *J. Hydrol.*, 517, 863–876, doi:10.1016/j.jhydrol.2014.06.009, 2014. 9067
- McKay, M. D., Beckman, R. J., and Conover, W. J.: A Comparison of Three Methods for Selecting Values of Input Variables in the Analysis of Output from a Computer Code, *Technometrics*, 21, 239–245, doi:10.2307/1268522, 1979. 9072
- Mesa, O. J. and Mifflin, E. R.: On the Relative Role of Hillslope and Network Geometry in Hydrologic Response, in: *Scale Problems in Hydrology*, vol. 6 of *Water Science and Technology Library*, edited by: Gupta, V. K., Rodríguez-Iturbe, I., and Wood, E. F., Springer Netherlands, 1–17, doi:10.1007/978-94-009-4678-1\_1, 1986. 9063
- Milly, P. C. D. and Shmakin, A. B.: Global modeling of land water and energy balances, Part I: The land dynamics (LaD) model, *J. Hydrometeorol.*, 3, 283–299, doi:10.1175/1525-7541(2002)003<0283:GMOLWA>2.0.CO;2, 2002. 9057
- Montgomery, D. R. and Foufoula-Georgiou, E.: Channel network source representation using digital elevation models, *Water Resour. Res.*, 29, 3925–3934, doi:10.1029/93WR02463, 1993. 9061
- Nash, J. E. and Sutcliffe, J. V.: River flow forecasting through conceptual models part I. A discussion of principles, *J. Hydrol.*, 10, 282–290, doi:10.1016/0022-1694(70)90255-6, 1970. 9072
- Nazemi, A. and Wheeler, H. S.: On inclusion of water resource management in Earth system models – Part 1: Problem definition and representation of water demand, *Hydrol. Earth Syst. Sci.*, 19, 33–61, doi:10.5194/hess-19-33-2015, 2015. 9057
- Nicotina, L., Alessi Celegon, E., Rinaldo, A., and Marani, M.: On the impact of rainfall patterns on the hydrologic response, *Water Resour. Res.*, 44, W12401, doi:10.1029/2007WR006654, 2008. 9065

# HESSD

12, 9055–9090, 2015

## HydroSCAPE: an innovative multi-scale routing model

S. Piccolroaz et al.

[Title Page](#)

[Abstract](#)

[Introduction](#)

[Conclusions](#)

[References](#)

[Tables](#)

[Figures](#)

[⏪](#)

[⏩](#)

[◀](#)

[▶](#)

[Back](#)

[Close](#)

[Full Screen / Esc](#)

[Printer-friendly Version](#)

[Interactive Discussion](#)

- Niu, G. Y., Yang, Z. L., Mitchell, K. E., Chen, F., Ek, M. B., Barlage, M., Kumar, A., Manning, K., Niyogi, D., Rosero, E., Tewari, M., and Xia, Y.: The community Noah land surface model with multiparameterization options (Noah-MP): 1. Model description and evaluation with local-scale measurements, *J. Geophys. Res.-Atmos.*, 116, D12109, doi:10.1029/2010JD015139, 2011. 9057
- O’Callaghan, J. F. and Mark, D. M.: The extraction of drainage networks from digital elevation data, *Comput. Vision Graph.*, 28, 323–344, 1984. 9068
- Oleson, K., Lawrence, D. M., Bonan, G. B., Drewniak, B., Huang, M., Koven, C. D., Levis, S., Li, F., Riley, W. J., Subin, Z. M., Swenson, S., Thornton, P. E., Bozbiyik, A., Fisher, R., Heald, C. L., Kluzek, E., Lamarque, J. F., Lawrence, P. J., Leung, L. R., Lipscomb, W., Muszala, S. P., Ricciuto, D. M., Sacks, W. J., Sun, Y., Tang, J., and Yang, Z. L.: Technical description of version 4.5 of the Community Land Model (CLM), NCAR Technical Note NCAR/TN-503+STR, Tech. rep., National Center for Atmospheric Research, Boulder, Colorado, USA, doi:10.5065/D6RR1W7M, 2013. 9057
- Prentice, I. C., Liang, X., Medlyn, B. E., and Wang, Y. P.: Reliable, robust and realistic: the three R’s of next-generation land-surface modelling, *Atmos. Chem. Phys.*, 15, 5987–6005, doi:10.5194/acp-15-5987-2015, 2015. 9057
- Rigon, R., Bancheri, M., Formetta, G., and de Lavenne, A.: The geomorphic unit hydrograph from a historical-critical perspective, *Earth Surf. Proc. Land.*, in review, 2015. 9066
- Rinaldo, A., Marani, A., and Rigon, R.: Geomorphological dispersion, *Water Resour. Res.*, 27, 513–525, doi:10.1029/90WR02501, 1991. 9057, 9060, 9063
- Rinaldo, A., Vogel, G. K., Rigon, R., and Rodriguez-Iturbe, I.: Can One Gauge the Shape of a Basin?, *Water Resour. Res.*, 31, 1119–1127, doi:10.1029/94WR03290, 1995. 9063
- Rinaldo, A., Botter, G., Bertuzzo, E., Uccelli, A., Settin, T., and Marani, M.: Transport at basin scales: 1. Theoretical framework, *Hydrol. Earth Syst. Sci.*, 10, 19–29, doi:10.5194/hess-10-19-2006, 2006. 9066
- Rodríguez-Iturbe, I. and Rinaldo, A.: *Fractal river basins: Chance and self-organization*, Cambridge University Press, Cambridge, UK, 1997. 9059, 9063, 9069
- Rubin, Y., Sun, A., Maxwell, R., and Bellin, A.: The concept of block-effective macrodispersivity and a unified approach for grid-scale- and plume-scale-dependent transport, *J. Fluid Mech.*, 395, 161–180, doi:10.1017/S0022112099005868, 1999. 9065

## HydroSCAPE: an innovative multi-scale routing model

S. Piccolroaz et al.

[Title Page](#)

[Abstract](#)

[Introduction](#)

[Conclusions](#)

[References](#)

[Tables](#)

[Figures](#)

[⏪](#)

[⏩](#)

[◀](#)

[▶](#)

[Back](#)

[Close](#)

[Full Screen / Esc](#)

[Printer-friendly Version](#)

[Interactive Discussion](#)



- Samaniego, L., Kumar, R., and Attinger, S.: Multiscale parameter regionalization of a grid-based hydrologic model at the mesoscale, *Water Resour. Res.*, 46, W05523, doi:10.1029/2008WR007327, 2010. 9057
- Sapriza-Azuri, G., Jódar, J., Navarro, V., Slooten, L. J., Carrera, J., and Gupta, H. V.: Impacts of rainfall spatial variability on hydrogeological response, *Water Resour. Res.*, 51, 1300–1314, doi:10.1002/2014WR016168, 2015. 9065
- Sivapalan, M.: Process complexity at hillslope scale, process simplicity at the watershed scale: is there a connection?, *Hydrol. Process.*, 17, 1037–1041, doi:10.1002/hyp.5109, 2003. 9060
- Tarboton, D. G., Bras, R. L., and Rodríguez-Iturbe, I.: On the extraction of channel networks from digital elevation data, *Hydrol. Process.*, 5, 81–100, doi:10.1002/hyp.3360050107, 1991. 9061, 9068
- US Soil Conservation Service: SCS National Engineering Handbook, vol. Hydrology, Sect. 4, US Department of Agriculture, Washington, D.C., 1964. 9062, 9069
- Van Beek, L. P. H., Wada, Y., and Bierkens, M. F. P.: Global monthly water stress: 1. Water balance and water availability, *Water Resour. Res.*, 47, W07517, doi:10.1029/2010WR009791, 2011. 9057
- van der Knijff, J. M., Younis, J., and de Roo, A. P. J.: LISFLOOD: A GIS-based distributed model for river basin scale water balance and flood simulation, *Int. J. Geogr. Inf. Sci.*, 24, 189–212, doi:10.1080/13658810802549154, 2010. 9057
- Van Der Tak, L. D. and Bras, R. L.: Incorporating hillslope effects into the geomorphologic instantaneous unit hydrograph, *Water Resour. Res.*, 26, 2393–2400, doi:10.1029/90WR00862, 1990. 9065
- Verzano, K., Bärlund, I., Flörke, M., Lehner, B., Kynast, E., Voß, F., and Alcamo, J.: Modeling variable river flow velocity on continental scale: Current situation and climate change impacts in Europe, *J. Hydrol.*, 424–425, 238–251, doi:10.1016/j.jhydrol.2012.01.005, 2012. 9058
- Volpi, E., Di Lazzaro, M., and Fiori, A.: A simplified framework for assessing the impact of rainfall spatial variability on the hydrologic response, *Adv. Water Resour.*, 46, 1–10, doi:10.1016/j.advwatres.2012.04.011, 2012. 9065
- Vörösmarty, C. J., Federer, C. A., and Schloss, A. L.: Potential evaporation functions compared on US watersheds: Possible implications for global-scale water balance and terrestrial ecosystem modeling, *J. Hydrol.*, 207, 147–169, doi:10.1016/S0022-1694(98)00109-7, 1998. 9057

# HESSD

12, 9055–9090, 2015

## HydroSCAPE: an innovative multi-scale routing model

S. Piccolroaz et al.

[Title Page](#)

[Abstract](#)

[Introduction](#)

[Conclusions](#)

[References](#)

[Tables](#)

[Figures](#)



[Back](#)

[Close](#)

[Full Screen / Esc](#)

[Printer-friendly Version](#)

[Interactive Discussion](#)



Wen, Z., Liang, X., and Yang, S.: A new multiscale routing framework and its evaluation for land surface modeling applications, *Water Resour. Res.*, 48, W08528, doi:10.1029/2011WR011337, 2012. 9059

Whiteaker, T. L., Maidment, D. R., Goodall, J. L., and Takamatsu, M.: Integrating arc hydro features with a schematic network, *Trans. GIS*, 10, 219–237, doi:10.1111/j.1467-9671.2006.00254.x, 2006. 9059

Widén-Nilsson, E., Halldin, S., and Xu, C. y.: Global water-balance modelling with WASMOD-M: Parameter estimation and regionalisation, *J. Hydrol.*, 340, 105–118, doi:10.1016/j.jhydrol.2007.04.002, 2007. 9057

Wood, E. F., Roundy, J. K., Troy, T. J., van Beek, L. P. H., Bierkens, M. F. P., Blyth, E., de Roo, A., Doell, P., Ek, M., Famiglietti, J., Gochis, D., van de Giesen, N., Houser, P., Jaffe, P. R., Kollet, S., Lehner, B., Lettenmaier, D. P., Peters-Lidard, C., Sivapalan, M., Sheffield, J., Wade, A., and Whitehead, P.: Hyperresolution global land surface modeling: Meeting a grand challenge for monitoring Earth's terrestrial water, *Water Resour. Res.*, 47, W05301, doi:10.1029/2010WR010090, 2011. 9058

Yamazaki, D., Kanae, S., Kim, H., and Oki, T.: A physically based description of floodplain inundation dynamics in a global river routing model, *Water Resour. Res.*, 47, W04501, doi:10.1029/2010WR009726, 2011. 9058

## HydroSCAPE: an innovative multi-scale routing model

S. Piccolroaz et al.

**Table 1.** Main geomorphic characteristics of the inter-basin drainage areas within the Upper Tiber river basin (CV: coefficient of variation).

Basin	ID	Area [km <sup>2</sup> ]	Slope [m m <sup>-1</sup> ]	Channel length statistics			
				Max [m]	Mean [m]	Variance [m <sup>2</sup> ]	CV [m m <sup>-1</sup> ]
Tiber at Santa Lucia	SL	932	0.009	69 660	32 482	$2.03 \times 10^8$	0.44
Tiber at Ponte Felcino	PF	2032	0.005	120 910	60 201	$6.97 \times 10^8$	0.44
Topino at Ponte Bettona	PB	1180	0.009	70 530	37 495	$2.41 \times 10^8$	0.41
Chiascio at Ponte Rosciano	PR	1909	0.007	100 440	48 477	$4.74 \times 10^8$	0.45
Tiber at Ponte Nuovo	PN	4116	0.005	144 110	67 410	$8.84 \times 10^8$	0.44

[Title Page](#)
[Abstract](#)
[Introduction](#)
[Conclusions](#)
[References](#)
[Tables](#)
[Figures](#)
[Back](#)
[Close](#)
[Full Screen / Esc](#)
[Printer-friendly Version](#)
[Interactive Discussion](#)




## HydroSCAPE: an innovative multi-scale routing model

S. Piccolroaz et al.

**Table 2.** Optimal model parameters, calibrated at Ponte Nuovo station (event February 1999), Nash–Sutcliffe efficiency indexes for Ponte Nuovo and all nodes, and computational time cost (for 100 000 runs) resulting from the calibration procedure, for different spatial scale resolutions (size of the macrocell).

Spatial scale	$n$ . macrocells	$V_c$ [m s <sup>-1</sup> ]	$c_s$ [-]	$\lambda$ [d]	NSE (PN) [-]	NSE (all nodes) [-]	comp. time [min]
5 km	476	2.18	1.23	0.30	0.99	0.64	10.2
10 km	126	2.19	1.17	0.29	0.99	0.69	3.00
50 km	6	2.43	1.05	0.30	0.97	0.56	0.44
150 km	1	2.26	0.83	0.22	0.94	-0.69	0.22

[Title Page](#)
[Abstract](#)
[Introduction](#)
[Conclusions](#)
[References](#)
[Tables](#)
[Figures](#)
[Back](#)
[Close](#)
[Full Screen / Esc](#)
[Printer-friendly Version](#)
[Interactive Discussion](#)


## HydroSCAPE: an innovative multi-scale routing model

S. Piccolroaz et al.

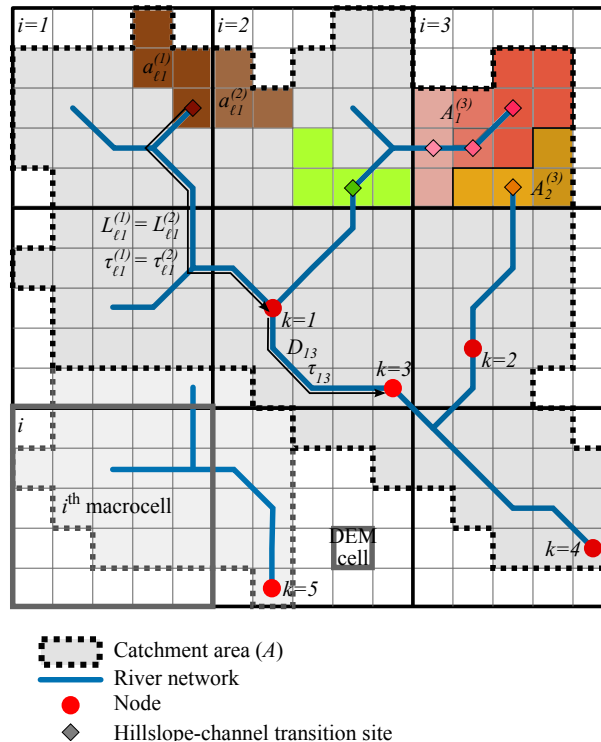


**Figure 1.** Sketch of basin conceptualization: subdivision of the study area into macrocells and nodes (red dots). River network is subdivided into hillslope-channel transition sites (colored squared symbols) each associated to a pertaining hillslope area  $a_{\ell k}^{(i)}$  (colored areas). For this simple case we consider  $N = 9$  macrocells and  $k = 5$  nodes. An example of two pathways characterized by the same length  $L_{\ell k}^{(i)}$  and travel time  $\tau_{\ell k}^{(i)}$  is also sketched.

Title Page

Abstract

Introduction

Conclusions

References

Tables

Figures

◀

▶

◀

▶

Back

Close

Full Screen / Esc

Printer-friendly Version

Interactive Discussion

## HydroSCAPE: an innovative multi-scale routing model

S. Piccolroaz et al.

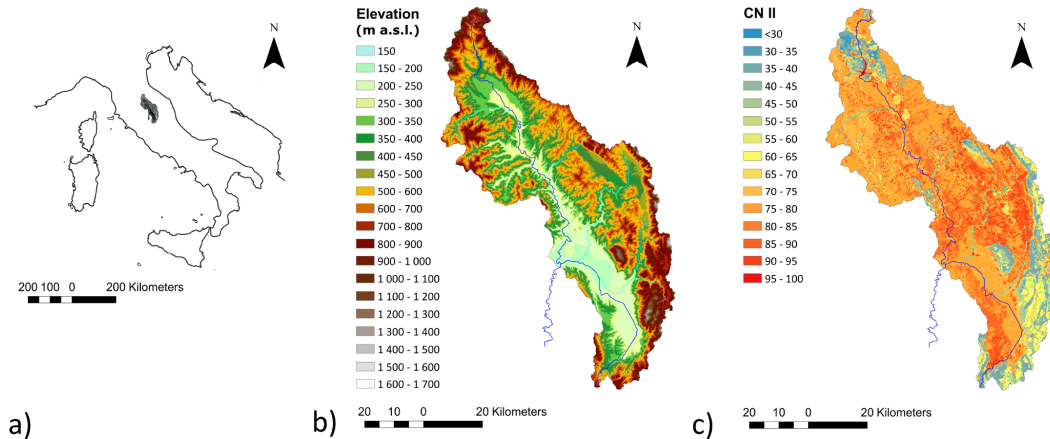


**Figure 2.** Maps showing: **(a)** the location of the Upper Tiber river basin within the Italian Peninsula, **(b)** DEM of the watershed and **(c)** fine scale land classification according to the CN II parameter.

Title Page

Abstract

Introduction

Conclusions

References

Tables

Figures

⏪

⏩

◀

▶

Back

Close

Full Screen / Esc

Printer-friendly Version

Interactive Discussion



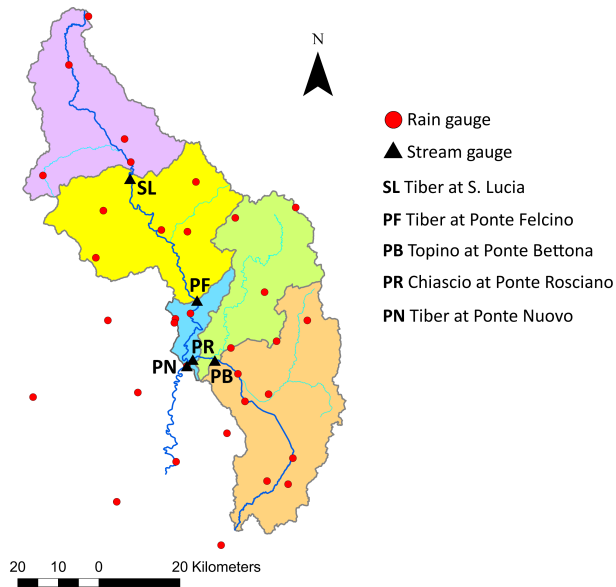


**Figure 3.** Map showing the subdivision of the watershed into 5 inter-basins, each one identified by a node where water discharge is computed (black triangles). The location of the meteorological stations are also shown as colored dots.

## HydroSCAPE: an innovative multi-scale routing model

S. Piccolroaz et al.

Title Page

Abstract

Introduction

Conclusions

References

Tables

Figures

⏪

⏩

◀

▶

Back

Close

Full Screen / Esc

Printer-friendly Version

Interactive Discussion



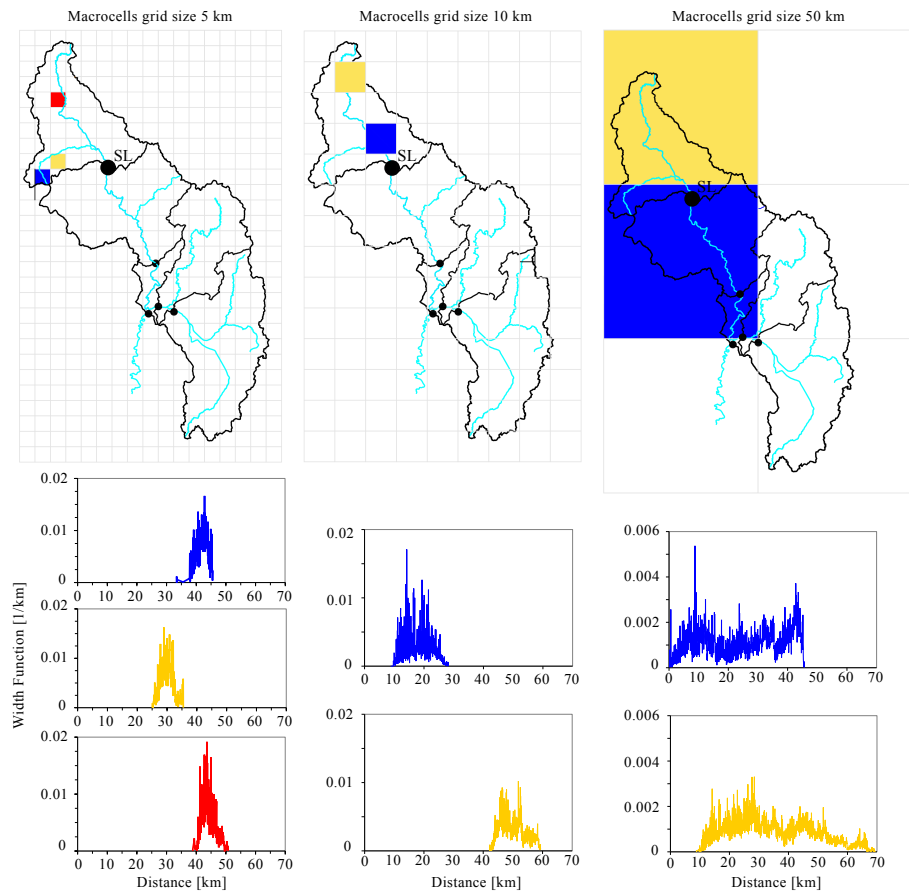


**Figure 4.** Macrocell width functions at the Santa Lucia (SL) control section for grid sizes of 5, 10 and 50 km. Colors indicates different macrocell-node combinations.

**HydroSCAPE: an innovative multi-scale routing model**

S. Piccolroaz et al.

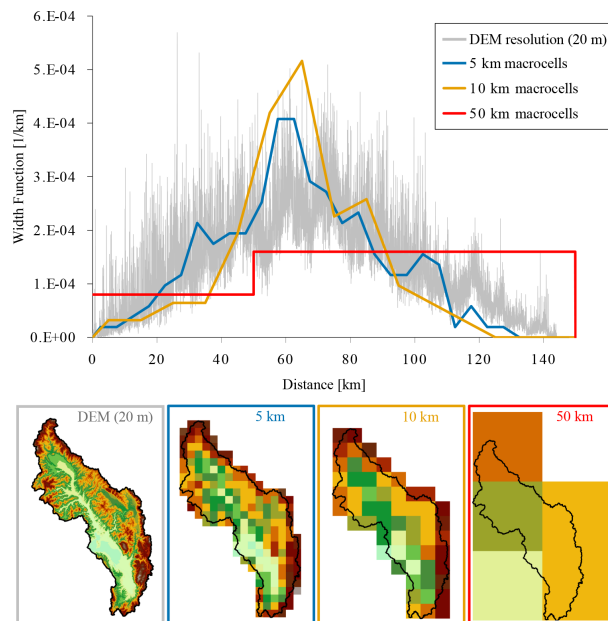


**Figure 5.** Width functions of the Upper Tiber river basin at Ponte Nuovo (PN) outlet (4116 km<sup>2</sup>) obtained aggregating the original 20 m DEM to 5 (blue), 10 (orange), and 50 (red) km. The width function derived from the original 20 m DEM is also shown (grey). Aggregated DEMs with grid size of 5, 10, and 50 km are shown in the lower part of the figure.

[Title Page](#)[Abstract](#)[Introduction](#)[Conclusions](#)[References](#)[Tables](#)[Figures](#)[Back](#)[Close](#)[Full Screen / Esc](#)[Printer-friendly Version](#)[Interactive Discussion](#)

## HydroSCAPE: an innovative multi-scale routing model

S. Piccolroaz et al.

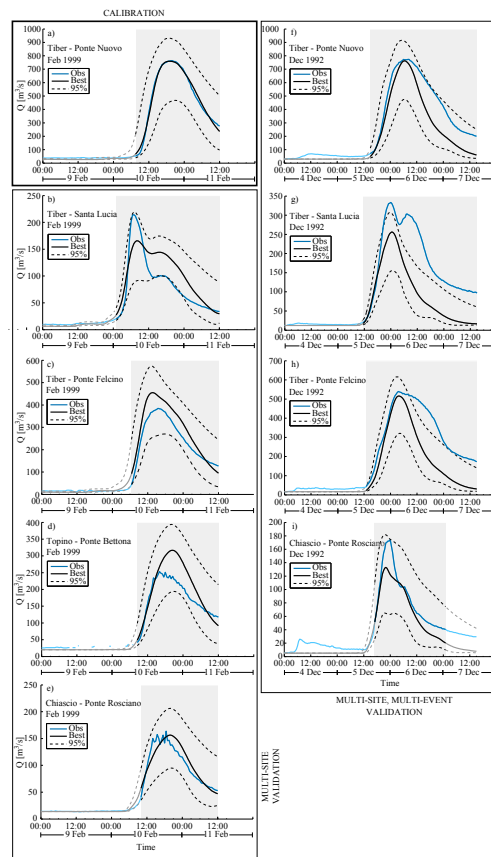


**Figure 6.** Comparison between 95 % confidence band, water discharge simulated with the optimal parameter set and observed at all the gauging stations and events: **(a)–(e)** 6–12 February 1999, and **(e)–(i)** 4–7 December 1992. Shaded areas identify the period considered in the evaluation of  $P$  and  $R$  factors. Model parameters are estimated by using the discharge at Ponte Nuovo (PN) measured during the 1999 event **(a)**.

Title Page

Abstract

Introduction

Conclusions

References

Tables

Figures

◀

▶

◀

▶

Back

Close

Full Screen / Esc

Printer-friendly Version

Interactive Discussion